Dalton Transactions

ROYAL SOCIETY OF CHEMISTRY

PAPER

View Article Online
View Journal | View Issue

Check for updates

Cite this: *Dalton Trans.*, 2025, **54**, 3057

Towards the photodeposition of Si_xGe_y-type materials *via* oligomers of cyclogermapentenes and cyclosilapentenes†

William Medroa del Pino, [a] Andres Forero Pico, [b] Abhishek V. Muralidharan, [a] Manisha Gupta [b] and Eric Rivard *[a]

Received 12th December 2024,
Accepted 8th January 2025

DOI: 10.1039/d4dt03446e

rsc.li/dalton

This article provides an alternative pathway towards cyclosilapentenes (*e.g.*, **SiH_2-^{i}Pr** and **SpiroSi**) involving the use of Rieke magnesium to activate the requisite dienes for synthesis. Subsequent metal-mediated dehydrocoupling of cyclosilapentene **SiH_2-^{i}Pr** and mixtures with another cyclogermapentene gives oligomers with backbone Si–Si (number average molecular weight, M_n = 1.0 kDa) and Si–Ge (M_n = 1.4 kDa) linkages, respectively. UV-irradiation (248 nm) of the abovementioned oligotetrelenes and the molecular spirosilane **SpiroSi** were examined in solution; while evidence for Si_xGe_y-type materials was noted through Raman and EDX spectroscopy, the presence of substantial amorphous carbon as a contaminant was also observed. (TD)-DFT computational studies on the spirosilane **SpiroSi** provide some insight into the lack of efficient Si_xGe_y photodeposition noted in this study.

Introduction

Silicon is the most widely used element in the production of electronic devices due to its low bandgap (1.1 eV) and its large-scale production.[1] Additionally, Si forms stable oxides when exposed to air, which enables its use in the fabrication of photolithographic masks.[1a,b] Silicon germanide (Si_xGe_y) is also a useful semiconductor due to the bandgap tuning that is possible through variation in the Si/Ge ratio. Likewise, Si_xGe_y exhibits exceptional thermoelectric properties.[2a] These features, alongside its resistance to extreme temperatures (up to 1000 °C) and radiation has prompted the use of Si_xGe_y in the fabrication of thermoelectrics, photodetectors, photodiodes, transistors, and photovoltaic cells.[2]

Despite all of the described advantages, standard routes towards Si and Si_xGe_y (*e.g.*, chemical vapor deposition, CVD) make use of toxic and sometimes corrosive chlorinated precursors, such as $HSiCl_3$. Furthermore, the need of high temperatures alongside sophisticated instrumentation makes these syntheses difficult to access for many.[3] Therefore, the development of more efficient techniques to deposit films of Si_xGe_y is highly desirable.

In previous work, we demonstrated the photopatterning of crystalline Ge films *via* the light-induced elimination of diene from poly(cyclogermapentene)s at room temperature.[4] Building on this approach, the present study shows the partially-successful photodeposition of Si and Si_xGe_y-type materials *via* UV-light irradiation of new tetrelene oligomers and a molecular spirosilane, albeit with carbon contamination. (TD)-DFT computations and stability assays on the photoextruded dienes are also discussed.

Results and discussion

Synthesis of Si and Si_xGe_y precursors

The initial step towards the attempted room temperature photodeposition of elemental Si and Si_xGe_y alloys involved the synthesis of the cyclic silanes 1,1-dihydro-3,4-di-iso-propylsilacyclopent-3-ene (**SiH_2-^{i}Pr**) and silaspiro-[4.4]-2,3,7,8-tetramethyl-2,7-nonadiene (**SpiroSi**) through a modified Rieke magnesium approach (Scheme 1a).[5] Characterization of both silanes by ^{1}H, ^{13}C{^{1}H}, and ^{29}Si{^{1}H} NMR spectroscopy showed the expected resonances for the assigned structures (Fig. S1–S6†). Additionally, high-resolution mass spectrometry (HR-MS) confirmed the presence of the molecular ion (M^+) in each product. Finally, FT-IR analysis of **SiH_2-^{i}Pr** supported the formation of a cyclic silane with an intense Si–H vibration centered at 2144 cm^{-1} (Fig. S22†).[6]

The synthesis of 1,1-dihydro-3,4-dibutylsilacyclopent-3-ene (**GeH_2-^{n}Bu**) was achieved *via* the cycloaddition of the dibutyl-

[a]*Department of Chemistry, University of Alberta, 11227 Saskatchewan Dr, Edmonton, Alberta, T6G 2G2, Canada. E-mail: erivard@ualberta.ca*
[b]*Department of Electrical Engineering, University of Alberta, 9211 116 St., Edmonton, Alberta, T6G 2H5, Canada. E-mail: mgupta1@ualberta.ca*

†Electronic supplementary information (ESI) available: Full experimental and computational details. See DOI: https://doi.org/10.1039/d4dt03446e

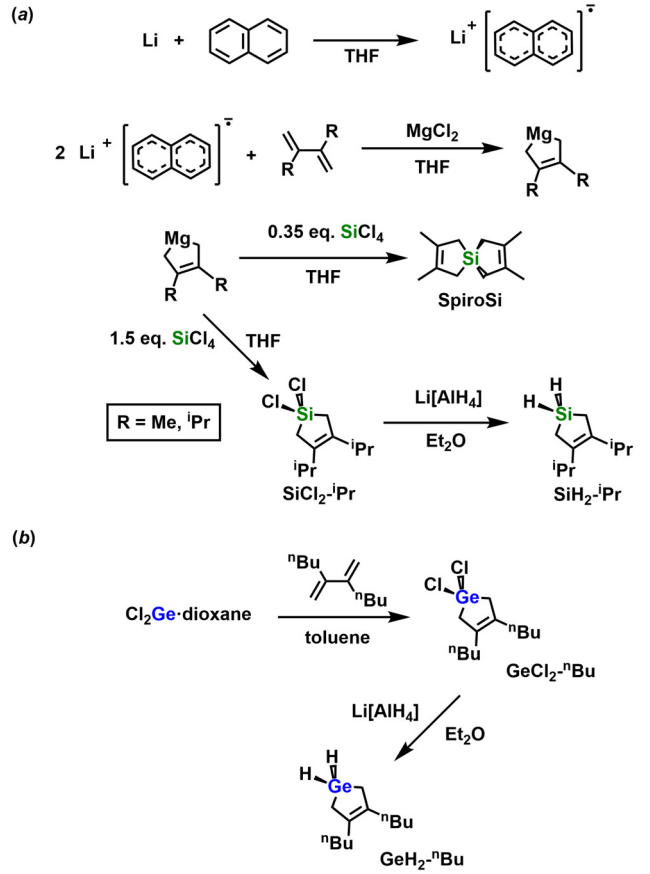

Scheme 1 (a) Synthesis of silaspiro-[4.4]-2,3,7,8-tetramethyl-2,7-nonadiene (**SpiroSi**) and 1,1-dihydro-3,4-di-iso-propylsilacyclopent-3-ene (**SiH_2-^{i}Pr**); (b) synthesis of 1,1-dichloro-3,4-dibutylgermacyclopent-3-ene **$GeCl_2$-^{n}Bu** and 1,1-dihydro-3,4-dibutylgermacyclopent-3-ene **GeH_2-^{n}Bu**.

ated diene (**diene-^{n}Bu**), $H_2C{=}C(^nBu){-}C(^nBu){=}CH_2$, with $Cl_2Ge{\cdot}$dioxane to first afford 1,1-dichloro-3,4-dibutylgermacyclopent-3-ene (**$GeCl_2$-^{n}Bu**). Halogen/hydride metathesis between **$GeCl_2$-^{n}Bu** and $Li[AlH_4]$ gave the expected germane **GeH_2-^{n}Bu** in 81% yield (Scheme 1b). The identities of **diene-^{n}Bu**, **$GeCl_2$-^{n}Bu**, and **GeH_2-^{n}Bu** were confirmed by ^{1}H and $^{13}C\{^1H\}$ NMR spectroscopies (Fig. S7–S12†), elemental analyses, and HR-MS.

The next step of this study involved the attempted dehydrocoupling polymerization of the silacyclopentene, **SiH_2-^{i}Pr**, using the known transition metal-based (pre-)catalysts $[Rh(COD)Cl]_2$, $[RhCl(PPh_3)_3]$, and $Cp_2Zr(pyr)(Me_3SiCCSiMe_3)$ (COD = cyclooctadiene; pyr = pyridine; Cp = η^5-C_5H_5).[7] Unexpectedly, analysis of the final reaction mixtures by ^{1}H NMR spectroscopy showed only partial monomer conversion with $[Rh(COD)Cl]_2$ or no reaction with $[RhCl(PPh_3)_3]$ or $Cp_2Zr(pyr)(Me_3SiCCSiMe_3)$. Despite changes in the catalyst loading from 0.1 to 2 mol%, the solvent employed (THF or toluene), the temperature of the reaction mixture (−30 °C, room temperature, or 70 °C), and time (1 to 7 days), no improvements were observed. Nevertheless, use of 0.1 mol% of $Pt(PCy_3)_2$ (Cy = cyclohexyl) as a dehydrocoupling catalyst[8] and heating to 60 °C without solvent led to observable bubbling (presumably H_2 formation) and the progressive coloration of the reaction mixture to light-yellow. Purification of the product by precipitation into MeCN (−30 °C) afforded a light-yellow semi-solid, **OligoSi**, in a yield of 58% (Scheme 2).

Characterization of **OligoSi** by Raman spectroscopy showed bands corresponding to the expected Si–Si, Si–C, and C=C stretches at 505, 880, and 1617 cm^{-1}, respectively.[6] Si–H stretches, expected at around 2100 cm^{-1}, were not observed (Fig. S23†). The Raman spectral data suggest the successful oligomerization to give a product with backbone Si–Si linkages and retention of the cyclosilapentene side units. Moreover, the absence of discernable Si–H units suggests the formation of linear chains of moderate molecular weight and/or generation of cyclic oligomers. ^{1}H NMR spectroscopic analysis of **OligoSi** showed broadened alkyl signals and the disappearance of the hydride peak from the monomer **SiH_2-^{i}Pr**; there is also a broad spectral feature around 5.3 ppm, assigned to Si–H end-groups (Fig. 1).[9]

Integration of the ^{1}H NMR alkyl signals and the Si–H peak in from **OligoSi** suggested the presence of *ca.* 10–11 repeating units, or a number average molecular weight (M_n) of 1.6 to 1.8 kDa. Likewise, gel permeation chromatography (GPC) in THF was also performed giving M_n = 1.0 kDa and a polydispersity index (PDI) of 2.3 (Fig. S34†). This analysis indicates the

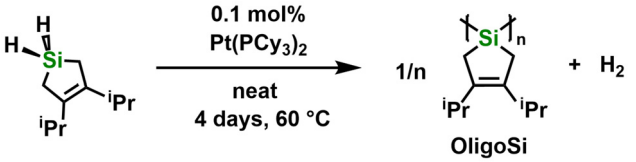

Scheme 2 Synthesis of oligo(3,4-di-iso-propylsilacyclopentene) (**OligoSi**).

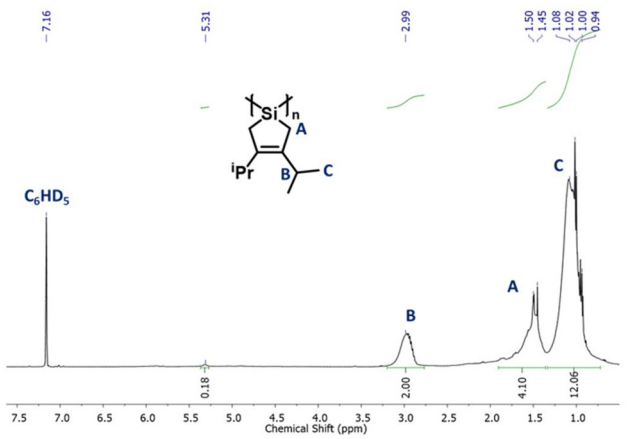

Fig. 1 ^{1}H NMR spectrum of oligo(3,4-di-iso-propylsilacyclopentene) (**OligoSi**) in C_6D_6.

formation of oligomers composed of 6 repeating units (on average), which correlates moderately well with the ^{1}H NMR end-group analysis, given the GPC instrumentation used. Thermogravimetric analysis (TGA) of **OligoSi** revealed an experimental weight loss of 60% upon heating to 500 °C; notably, this value is higher than the overall expected weight loss expected if only Si metal were to remain (83%) (Fig. S26†). Multiple TGA measurements using different samples of **OligoSi** were attempted, showing similar weight loss in each case.

Dehydrocoupling of **GeH$_2$-^{n}Bu** was also accomplished using 6 mol% of Pt(PCy$_3$)$_2$ in benzene at room temperature with continuous stirring under inert atmosphere for 18 hours. As with the synthesis of **OligoSi**, bubbling and the progressive coloration of the reaction mixture to light-yellow were observed. Purification of the product by precipitation from a concentrated solution in THF into cold MeCN (−30 °C) afforded **OligoGe** as a light-yellow semi-solid. Characterization of **OligoGe** by ^{1}H NMR spectroscopy showed the expected signal broadening and the disappearance of the GeH$_2$ resonance from **GeH$_2$-^{n}Bu**; in place, a broad resonance spanning 4.54 to 4.82 ppm was present, likely due to Ge–H end groups (Fig. S14†). Moreover, Raman spectroscopic analysis of this product supported the successful dehydrocoupling polymerization of **GeH$_2$-^{n}Bu** as a Ge–Ge stretch was present at 300 cm^{-1} along with a small band corresponding to a Ge–H stretch (end groups) at 2021 cm^{-1} (Fig. S24†).[6] As with **OligoSi**, the molecular weight of **OligoGe** was estimated by ^{1}H NMR end-group analysis and GPC, with the latter method giving M_n = 1.4 kDa and a PDI of 1.2, indicating the formation of oligomers with *ca.* 6 repeat units on average (Fig. S35†). TGA of **OligoGe** showed weight loss to a final remaining value of 35% upon heating to 400 °C, which is close in value to the expected remaining weight for the formation of elemental Ge (32%; Fig. S27†).

The successful dehydrocoupling of both **GeH$_2$-^{n}Bu** and **SiH$_2$-^{i}Pr** enabled the latter co-oligomerization of both monomers to form a possible Si/Ge photolithographic precursor to Si$_x$Ge$_y$. Note: different heterocyclic side groups (^{n}Bu and ^{i}Pr) were used for each monomer to enable determination of Si/Ge element ratios in the final oligomer by ^{1}H NMR spectroscopy. Upon addition of 2 mol% of Pt(PCy$_3$)$_2$ to a 1 : 1 mixture of **GeH$_2$-^{n}Bu** and **SiH$_2$-^{i}Pr** at 80 °C (in toluene) immediate bubbling and the progressive color change of the reaction mixture to light-orange were observed. After stirring for 18 h, thickening of the solution was noted until a light-orange viscous mixture remained. Purification of the product was accomplished by precipitation from THF into cold MeCN (−30 °C) to give **OligoSiGe** as an orange semi-solid (Scheme 3). Thermogravimetric analysis (TGA) of **OligoSiGe** under argon (Fig. S28†) showed a weight loss value of 68% upon heating to 400 °C; for comparison, the expected weight loss if only Si and Ge remained in a 1 : 1 ratio is 75%.

The ^{1}H NMR spectrum of **OligoSiGe** confirms the successful dehydrocoupling co-polymerization of **GeH$_2$-^{n}Bu** and **SiH$_2$-^{i}Pr**, as evidenced by the appearance of broad alkyl signals

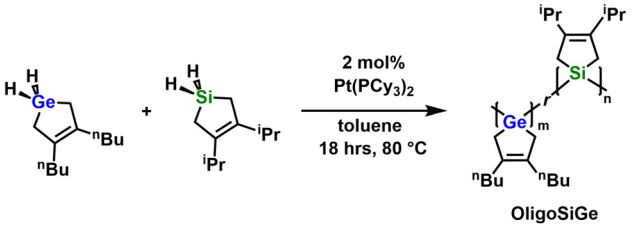

Scheme 3 Synthesis of oligo(3,4-dibutylgermacyclopentene-*r*-3,4-di-iso-propylsilacyclopentene) (**OligoSiGe**).

alongside the disappearance of the Si–H and Ge–H peaks from the monomers at 4.10 and 4.12 ppm, respectively. Likewise, the formation of new broad set of signals from 4.27 to 5.35 ppm suggested the presence of new silicon/germanium hydride end-groups (Fig. 2). Integration of the alkyl signals revealed an ^{i}Pr/^{n}Bu subunit ratio of 51/49, which matches closely with the 1 : 1 silane/germane monomer feed ratio used in the dehydrocoupling oligomerization. The Raman spectrum of **OligoSiGe** further supported the formation of this co-oligomer with discernable Ge–Ge, Si–Si, Si–Ge, Si–C, C=C, Ge–H, and Si–H stretches at 304, 463, 563, 878, 1622, 1997, and 2116 cm^{-1}, respectively (Fig. S25†).[6] End-group analysis of the alkyl and hydride ^{1}H NMR resonances in **OligoSiGe** gave an overall degree of polymerization of approximately 13 (M_n = 2.8 kDa). GPC analysis of **OligoSiGe** in THF was then performed, giving a number average molecular weight of 1.4 kDa, suggesting 7 repeating units per chain, and a PDI of 1.2 (Fig. S36†).

The above data point to the presence of low molecular weight oligomers for **OligoSi**, **OligoGe**, and **OligoSiGe**. These experimental results align with a related study by Tanaka and co-workers, who used Pt(COD)$_2$ as a pre-catalyst to synthesize silacyclopentane oligomers with a M_n value of 0.8 kDa, equivalent to 9 repeating units.[10]

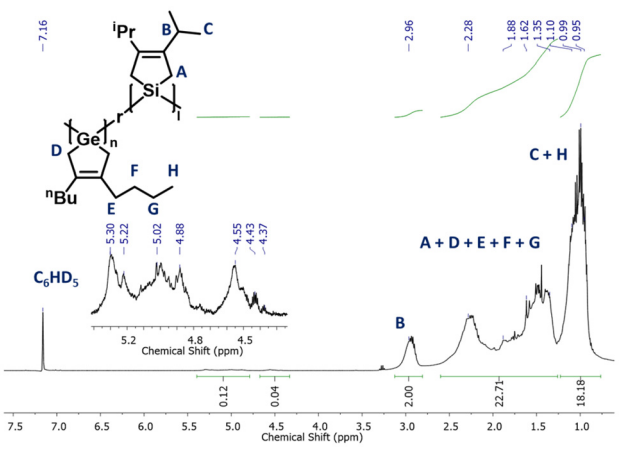

Fig. 2 ^{1}H NMR spectrum of oligo(3,4-dibutylgermacyclopentene-*r*-3,4-di-iso-propylsilacyclopentene) (**OligoSiGe**) in C$_6$D$_6$.

Photodeposition attempts

In order to determine the light absorption properties of the new Si/Ge oligomers reported here, UV-Vis spectra were recorded (Fig. S30–S33†). The UV-Vis spectrum of **OligoSi** in THF indicated no clear maxima in the range of 220–800 nm, but an absorption onset was observed at 310 nm. The spectrum of **OligoGe** gave an absorption maximum at 290 nm with a red-shifted onset of absorption at 336 nm. The UV-Vis spectrum of **OligoSiGe** in THF showed a similar absorption profile as **OligoSi**, with no discernible maxima and an absorption onset at 316 nm. Finally, the UV-Vis spectrum of the spirocyclic silane **SpiroSi** gave an absorption onset of 304 nm. These findings suggest that **OligoSi**, **OligoSiGe**, and **SpiroSi** are susceptible to irradiation by UV light with wavelengths below *ca.* 300 nm.

Photodeposition involving **OligoSi** was then attempted with irradiation from a 248 nm laser into a solution of the oligosilane in THF-d_8 at room temperature, using a custom-built[4] quartz reactor (Scheme 4).

As the photolysis of **OligoSi** proceeded, the color of the solution changed from colorless to light-yellow, and a dark solid started to form on the inner walls of the quartz reactor (Fig. 3). Unfortunately, the mass of the dark precipitate that also formed on the bottom of the reactor was too low for an accurate yield determination (<0.1 mg). ^{1}H NMR spectroscopic analysis of the reaction mixture after exposing **OligoSi** to UV light (in THF-d_8) showed oligosilane starting material along with small signals corresponding to 2,3-di-iso-propyl-1,3-butadiene (5%), confirming that the partial reverse cycloaddition of diene from **OligoSi** had occurred (Fig. 4). Surprisingly, analysis of the deposited inner grey-layer of the quartz reactor by Raman spectroscopy showed intense bands at 1585, 1326, and 1173 cm^{-1}, corresponding to amorphous carbon, and a weak signal at 493 cm^{-1} that could be assigned to Si–Si stretches (Fig. S38†).[6,11]

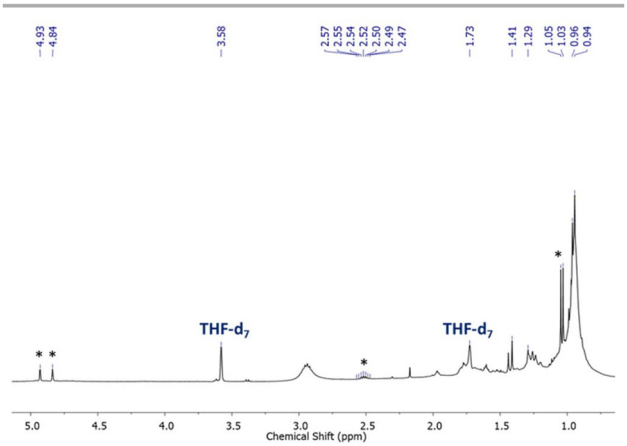

Fig. 4 ^{1}H NMR spectrum of the reaction mixture after photolysis of oligo(3,4-di-iso-propylsilacyclopentene) (**OligoSi**) in THF-d_8. Signals marked with (*) at 4.93, 4.84, 2.52, and 1.04 ppm correspond to the free diene, 2,3-di-iso-propyl-1,3-butadiene (**diene-^{i}Pr**).

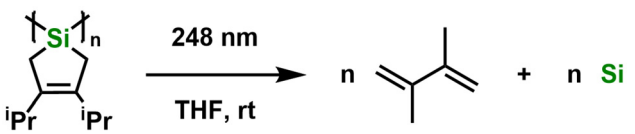

Scheme 4 Targeted photolysis of oligo(3,4-di-iso-propylsilacyclopentene) (**OligoSi**).

The deposited layer on the quartz reactor from the photolysis of **OligoSi** was also characterized by scanning electron microscopy (SEM), revealing irregular morphologies (Fig. S39†). Moreover, energy dispersive X-ray (EDX) analysis of this thin film indicated a high atomic carbon content (44.36%), further supporting the formation of amorphous carbon-based material during photolysis (Fig. S40†). It should be noted that detection of Si by EDX is unreliable in this case as the grey thin film was deposited on a quartz substrate. Finally, EDX analysis often presents background C contamination in our instrument, however, the carbon content observed for the thin film produced by the photolysis of **OligoSi** is significantly higher than what would be expected from background carbon alone.

Photodeposition of Si_xGe_y from **OligoSiGe** was also attempted using similar conditions as those employed for the photolysis experiments with **OligoSi**. As observed in previous experiments, a thin-layer of a dark-grey precipitate formed on the inner wall of the quartz reactor after the UV-light irradiation of **OligoSiGe** in THF at 248 nm (Fig. 5). ^{1}H NMR characterization of the remaining solution in THF-d_8 after

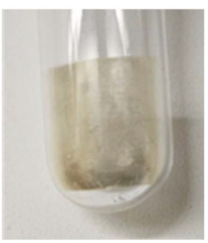

Fig. 3 Photograph of the deposited powder after photolysis of oligo (3,4-di-iso-propylsilacyclopentene) (**OligoSi**) in THF.

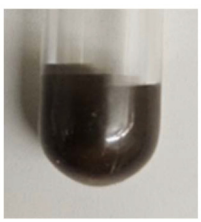

Fig. 5 Photograph of the deposited Si_xGe_y film (and carbon) after photolysis of oligo(3,4-dibutylgermacyclopentene-*r*-3,4-di-iso-propylsilacyclopentene) (**OligoSiGe**) in THF-d_8.

photolysis revealed broad signals corresponding to unreacted **OligoSiGe**. Nonetheless, low intensity peaks belonging to the expected dienes $H_2C{=}C(R){-}C(R){=}CH_2$ (R = ^{n}Bu and ^{i}Pr; ^{n}Bu = 8% and ^{i}Pr = 4%) were also observed (Fig. S17†).

The Raman spectrum of the deposited insoluble material from the photolysis of **OligoSiGe** shows a vibration at 298 cm^{-1}, due to Ge–Ge stretches, and a less intense/broader band between 410–506 cm^{-1}. This latter band likely corresponds to a combination of Si–Ge and Si–Si stretches, typically observed around 400 and 500 cm^{-1}, respectively.[6] These results indicate the successful deposition of a solid with some local Si_xGe_y structure. Finally, as observed in the photolysis of **OligoSi**, intense bands at 1173, 1327, and 1586 cm^{-1} were noted (Fig. 6), which match the Raman spectrum of amorphous carbon,[11] pointing to the partial decomposition of the organic by-products formed during the photolysis.

SEM and EDX data were also collected on the fine dark-grey powder obtained during the photolysis reaction of **OligoSiGe**. The SEM image of the precipitate, deposited onto carbon tape prior to analysis, revealed the formation of granules (Fig. S43†); EDX mapping of the material indicated presence of Ge and Si at 14.47 and 8.50 atomic%, respectively (Fig. S44†). These results suggest the formation of a bulk material with a Si/Ge ratio of approximately $Si_{0.37}Ge_{0.63}$.

To gain further insight into the results obtained from the photodeposition attempts of **OligoSi** and **OligoSiGe**, photolysis experiments using **SpiroSi** were also conducted in cyclohexane-d_{12} under a nitrogen atmosphere at room temperature. Similar to the photolysis of **OligoSi**, a fine layer of a grey solid was formed on the inner surface of the quartz reactor and the initially colorless solution adopted a deep yellow color after completion of 10 000 light pulses (Fig. 7). The photolysis of **SpiroSi** was also attempted in THF-d_8 to probe the influence of a more polar solvent on the reaction outcome. As before, coloration to deep yellow and the formation of a small amount of a black precipitate were observed. These results indicate that formation of the carbon contaminant is not influenced substantially by the solvent employed. Analysis of the reaction mixture using ^{1}H NMR spectroscopy indicated a significant amount of unreacted **SpiroSi**. Additionally, signals corresponding to 2,3-dimethyl-1,3-butadiene (**diene-Me**) were also detected at 5.05, 4.94, and 1.89 ppm, suggesting the partially successful reverse-cycloaddition of diene from the **SpiroSi** (Fig. S18†).

SEM analysis of the recovered dark-grey precipitate obtained from the photolysis of **SpiroSi** showed an uneven solid (Fig. 8a). EDX characterization revealed a high carbon content (73.57%) and only a small atomic percentage of Si (6.02%) (Fig. 8b). These findings suggest that irradiation of **SpiroSi** with UV light leads to the decomposition of the organic fraction(s) leading to amorphous carbon, as observed with the photolysis of **OligoSi** and **OligoSiGe**.

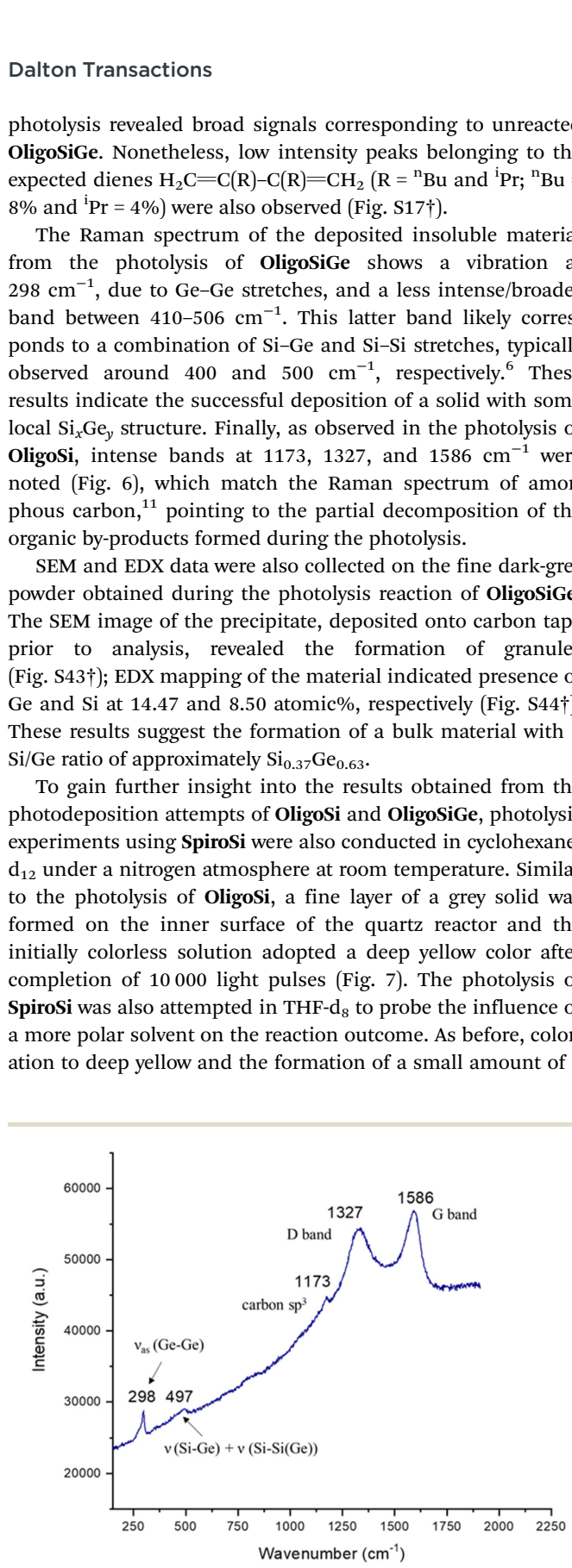

Fig. 6 Raman spectrum of the dark-grey film obtained from the photolysis of oligo(3,4-dibutylgermacyclopentene-*r*-3,4-di-iso-propylsilacyclopentene) (**OligoSiGe**).

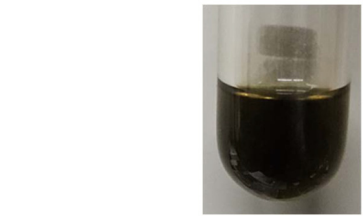

Fig. 7 Photograph of the reaction mixture after photolysis of silaspiro-[4.4]-2,3,7,8-tetramethyl-2,7-nonadiene (**SpiroSi**) in cyclohexane-d_{12}.

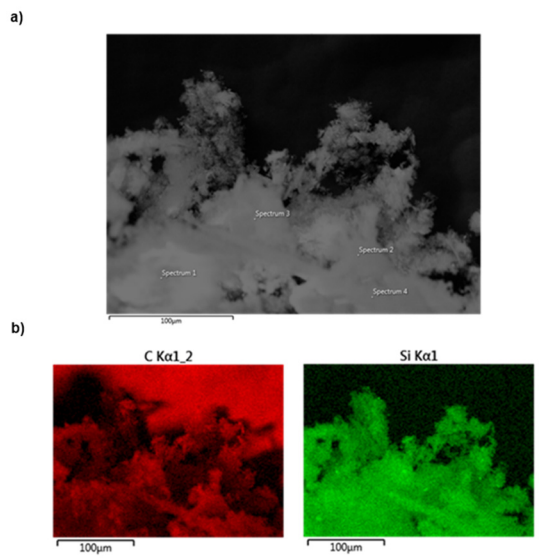

Fig. 8 (a) SEM backscattered-electron image for the dark-grey precipitate obtained from the photolysis of silaspiro-[4.4]-2,3,7,8-tetramethyl-2,7-nonadiene (**SpiroSi**); SEM data was collected at 15 keV; (b) EDX elemental maps for the dark-grey precipitate obtained from the photolysis of silaspiro-[4.4]-2,3,7,8-tetramethyl-2,7-nonadiene (**SpiroSi**) in THF.

Photostability studies involving dienes

The presence of amorphous carbon after the photolysis of **OligoSi**, **OligoSiGe**, and **SpiroSi** led an evaluation of the stability of the corresponding diene by-products under UV-light. In this regard, solutions of $H_2C{=}C(R){-}C(R){=}CH_2$ (R = **Me**, **^{i}Pr**, **^{n}Bu**) in dry THF were irradiated with a KrF laser at 248 nm, following the same conditions as employed in the abovementioned photolysis experiments. The colorless solution of the **diene-^{i}Pr** changed rapidly to a light-yellow tone once irradiation began, as observed with **OligoSi** and **SpiroSi**. Additionally, traces of a dark-grey precipitate formed on the inner wall of the quartz reactor, albeit in lower quantities than observed with the Ge and Si oligomers (Fig. 9a). In contrast, solutions of **diene-Me** and **diene-^{n}Bu** in THF showed no visible change after exposure to UV light (Fig. 9b and c).

^{1}H NMR spectroscopic analysis of the THF-d_8 solutions of **diene-^{i}Pr**, **diene-Me**, and **diene-^{n}Bu** after photolysis revealed the formation of some unknown signals, along with unreacted butadienes (Fig. S19–S21†). It is salient to mention here prior work by Traetteberg and co-workers, who observed the rearrangement of the bulky diene 2,3-di-*tert*-buyl-1,3-butadiene into an unsymmetric cyclobutene upon irradiation with a high-pressure Hg lamp (356 nm) at room temperature;[12] note, the authors did not report the formation of insoluble precipitates during their photolysis experiments.

The photolysis of **diene-^{i}Pr**, **diene-Me**, and **diene-^{n}Bu** alongside the study conducted by Traetteberg show the susceptibility of alkylated-dienes towards UV-light. However, the generation of the amorphous carbon in our abovementioned studies suggests further degradation of any possible diene-rearrangement product(s) had transpired. Of note, our photolysis studies involving the free dienes **OligoSi**, **SpiroSi**, and **OligoSiGe** were conducted at room temperature. However, during irradiation the reaction mixtures undergo significant heating (to *ca.* 50 °C) due to the intense energy supplied by the laser, requiring a cooling period of five minutes after every 2500 pulses to return to room temperature. In contrast, Traetteberg and co-workers conducted their photolysis studies at room temperature; also, it is possible that their use of a lower wavelength (356 nm) light source might have prevented further degradation of their soluble products. Moreover, Traetteberg[12] employed a Hg lamp for their irradiation experiments, while our study used more intense and a higher energy (248 nm) excimer KrF laser. Finally, our previous work involving the photopatterning of elemental Ge from poly(cyclogermapentene)s, employing **diene-^{i}Pr**, **diene-^{n}hexyl**, and **diene-Me** as organic moieties, did not show presence of carbon contamination in the Raman spectra of the deposited films.[4] One possible explanation for this is the more rapid decomposition of the Ge polymers in this prior work, leading to formation of Ge films that block further UV-light from reaching the dienes formed; thus, preventing the generation of amorphous carbon.

TD-DFT computations on SpiroSi

To gain a better understanding of the UV-vis transition(s) available when **SpiroSi** is exposed to UV-light, time-dependent density functional theory (TD-DFT) computations at the B3LYP/cc-pVDZ[13] level, as well as standard DFT calculations, were performed (Fig. 10). The computed UV-vis spectrum (Fig. S49†) for **SpiroSi** reveals an intense absorption at 185 nm, driven by an electronic transition between the HOMO (C–C π) and the LUMO (C–C π*). Nonetheless, a minor intensity transition that could potentially induce the reverse cycloaddition of diene from Si is computed at 176 nm, corresponding to the excitation between the HOMO−2 (of Si–C σ-character) and the LUMO (C–C π*) (Table S1†). Unfortunately, the oscillator strength for this transition is only 0.0002, making the process exceedingly inefficient (Table S1†). Thus, the experimentally employed excitation wavelength (248 nm) is likely responsible for the low yield of photoextruded products (diene and insoluble solids) noted.

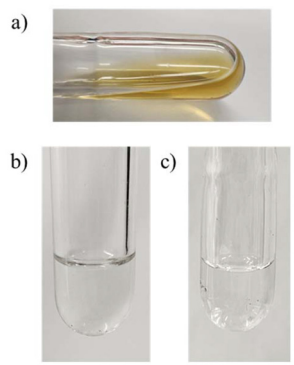

Fig. 9 (a) Solution of **diene-^{i}Pr** after photolysis at room temperature in THF; (b) solution of **diene-Me** after photolysis at room temperature in THF; (c) solution of **diene-^{n}Bu** after photolysis reaction at room temperature in THF. All three solutions were irradiated with a 248 nm KrF laser (15 Hz, 11 000 pulses, 230 mJ per pulse).

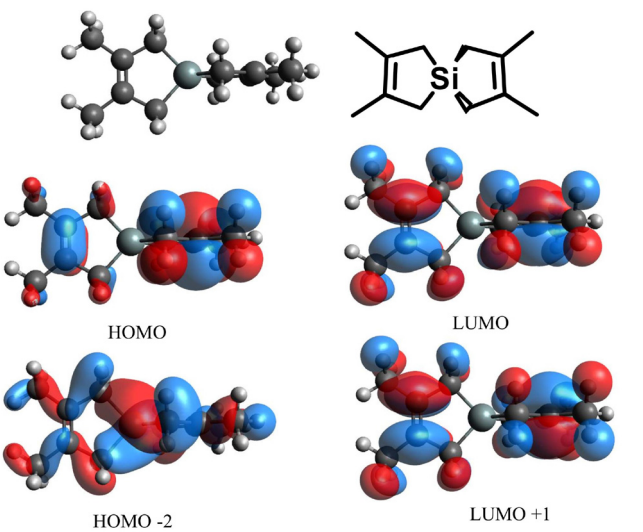

Fig. 10 Geometry optimization of $Si\{CH_2C(Me){=}C(Me)CH_2\}_2$ (**SpiroSi**) in the gas phase, and the computed frontier molecular orbitals at the B3LYP/cc-pVDZ level of theory.

The abovementioned computational studies on **SpiroSi** alongside the experimental data from the photolysis of **SpiroSi**, **OligoSi**, and **OligoSiGe** suggest that some photodeposition of Si_xGe_y-type materials could be possible *via* the reverse cycloaddition of diene. However, the formation of carbon contaminants during irradiation and the extremely low photodeposition reaction rate limit the applicability of this method to date. In this context, computations on **SpiroSi**, along with previous studies done by Traetteberg, as well as the experimental irradiation assays on **diene-Me**, **diene-^{n}Bu**, and **diene-^{i}Pr**, offer hints to overcome some of these challenges. First, the temperature at which the photolysis experiments is conducted could be key to preventing the formation of amorphous carbon from diene degradation. Thus, future experiments should employ a cooling bath (*ca.* 0 °C) during the photolysis. Unfortunately, our current laser set-up does not allow such temperature control. Secondly, a higher-energy/lower wavelength UV-light source[14] is likely required to enhance the rate of Si_xGe_y-type material deposition. In this regard, there are no suitable organic solvents in the literature with a UV absorption cut-off below 190 nm, indicating that further experiments following our methodology would need to be attempted without solvent (*i.e.*, in the bulk/film state).

Conclusions

The present work introduces an alternative synthesis of cyclosilapentadienes (**SiH_2-^{i}Pr** and **SpiroSi**). Dehydrocoupling oligomerization of **SiH_2-^{i}Pr** was possible to give the oligosilane **OligoSi**; co-oligomerization of **SiH_2-^{i}Pr** and **GeH_2-^{n}Bu** afforded **OligoSiGe**. Efforts to photodeposit Si and Si_xGe_y from **SpiroSi**, **OligoSi**, and **OligoSiGe** were explored with a 248 nm laser in THF. While evidence for the expected loss of diene was noted (albeit in low yield), the final Si_xGe_y-type products were contaminated with amorphous carbon. Future work will involve monomer modification to encourage more efficient photoextusion of diene from Si-containing heterocyclic precursors and extension of this element-extrusion process to other areas of the Periodic Table. Overall, this work represents a new chapter in the use of inorganic polymers as precursors to bulk semiconducting materials under mild, non-CVD, conditions.

Data availability

The data supporting this article have been included as part of the ESI.†

Conflicts of interest

There are no conflicts to declare.

Acknowledgements

E. R. thanks NSERC of Canada for Discovery and Accelerator Grants, and M. G. would like to acknowledge CFI JELF for funding. The authors would like to thank the following undergraduates for their experimental contributions to the manuscript: Long Dao and Mauricio Toshio Ito Tohara (synthesis of **diene-^{i}Pr**, **diene-^{n}Bu**, and **SiH_2-^{i}Pr**).

References

1 (*a*) E. E. Haller, *Mater. Sci. Semicond. Process.*, 2006, **9**, 408; (*b*) *Reference Module in Chemistry, Molecular Sciences and Chemical Engineering*, ed. N. Farahi, D. Y. N. Truong, H. Kleinke, X. Zhang, X. Zhang and J. Reedijk, Elsevier, 2016; (*c*) P. Geng, W. Li, X. Zhang, Y. Deng and H. Kou, *J. Phys. D: Appl. Phys.*, 2017, **50**, 40LT02; (*d*) *Handbook of Silicon Based MEMS Materials and Technologies*, ed. M. Tilli, M. Paulasto-Krockel, T. Motooka and V. Lindroos, Elsevier, 2020; (*e*) A. V. Shah, R. Platz and H. Keppner, *Sol. Energy Mater. Sol. Cells*, 1995, **38**, 501; (*f*) *Semiconductors for Room Temperature Nuclear Detector Applications*, ed. A. C. Beer, R. K. Willardson and E. R. Weber, Elsevier, 1995.

2 (*a*) B. Cook, *Energies*, 2022, **15**, 2957; (*b*) E. M. T. Fadaly, A. Dijkstra, J. R. Suckert, D. Ziss, M. A. J. van Tilburg, C. Mao, Y. Ren, V. T. van Lange, K. Korzun, S. Kölling, M. A. Verheijen, D. Busse, C. Rödl, J. Furthmüller, F. Bechstedt, J. Stangl, J. J. Finley, S. Botti, J. E. M. Haverkort and E. P. A. M. Bakkers, *Nature*, 2020, **580**, 205; (*c*) D. J. Paul, *Semicond. Sci. Technol.*, 2004, **19**, 75; (*d*) M. Arienzo, S. S. Iyer, B. S. Meyerson, G. L. Patton and J. M. C. Stork, *Appl. Surf. Sci.*, 1991, **48**, 377; (*e*) D. L. Harame, S. J. Koester, G. Freeman, P. Cottrel, K. Rim, G. Dehlinger, D. Ahlgren, J. S. Dunn, D. Greenberg, A. Joseph, F. Anderson, J.-S. Rieh, S. A. S. T. Onge, D. Coolbaugh, V. Ramachandran, J. D. Cressler and S. Subbanna, *Appl. Surf. Sci.*, 2004, **224**, 9.

3 (*a*) *Silicon–Germanium (SiGe) Nanostructures*, ed. Y. Shiraiki and N. Usami, Woodhead Publishing, 2011; (*b*) M. Gerwig, U. Böhme and M. Friebel, *Chem. – Eur. J.*, 2024, **33**, e202400013; (*c*) D.-S. Byeon, C. Cho, D. Yoon, Y. Choi, K. Lee, S. Baik and D. H. Ko, *Coatings*, 2021, **11**, 568; (*d*) A. A. Lovtsus, A. S. Segal, A. P. Sid'ko, R. A. Talalaev, P. Storck and L. Kadinski, *J. Cryst. Growth*, 2006, **287**, 446.

4 W. Medroa del Pino, A. A. Forero Pico, M. Gupta and E. Rivard, *Chem. Commun.*, 2023, **59**, 6849.

5 H. Xiong and R. D. Rieke, *J. Org. Chem.*, 1989, **54**, 3247.

6 (*a*) S. Tasleem, A. Sabah, M. Tahir, A. Sabir, A. Shabbir and M. Nazir, *ACS Omega*, 2022, **7**, 3940; (*b*) C. X. Cui and M. Kertesz, *Macromolecules*, 1992, **25**, 1103; (*c*) P. Vora, S. A. Solin and P. John, *Phys. Rev. B: Condens. Matter Mater. Phys.*, 1984, **29**, 3423; (*d*) S. A. Mala, L. Tsybeskov, D. J. Lockwood, X. Wu and J.-M. Baribeau, *J. Appl. Phys.*, 2014, **116**, 014305; (*e*) H. Li, I. S. Butler and J. F. Harrod, *Appl. Spectrosc.*, 1993, **47**, 1571.

7 (*a*) B. J. Grimmond and J. Y. Corey, *Organometallics*, 1999, **18**, 2223; (*b*) F. Fang, Q. Jiang and R. S. Klausen, *J. Am. Chem. Soc.*, 2022, **144**, 7834; (*c*) H.-G. Woo, J. F. Walzer and T. D. Tilley, *J. Am. Chem. Soc.*, 1992, **114**, 7047; (*d*) U. Rosenthal, *Organometallics*, 2020, **39**, 4403.

8 M. Garçon, C. Bakewell, G. A. Sackman, A. J. P. White, R. I. Cooper, A. J. Edwards and M. R. Crimmin, *Nature*, 2019, **574**, 390.

9 A. A. Omaña, R. K. Green, R. Kobayashi, Y. He, E. R. Antoniuk, M. J. Ferguson, Y. Zhou, J. G. C. Veinot, T. Iwamoto, A. Brown and E. Rivard, *Angew. Chem., Int. Ed.*, 2021, **60**, 228.

10 B. P. S. Chauhan, T. Shimizu and M. Tanaka, *Chem. Lett.*, 1997, **26**, 785.

11 S. Katz, A. Pevzner, V. Shepelev, S. Marx, H. Rotter, T. Amitay-Rosen and I. Nir, *MRS Adv.*, 2022, **7**, 245.

12 H. Hopf, H. Lipka and M. Traetteberg, *Angew. Chem., Int. Ed. Engl.*, 1994, **33**, 204.

13 (*a*) J. P. Perdew, K. Burke and M. Ernzerhof, *Phys. Rev. Lett.*, 1996, **77**, 3865; (*b*) T. H. Dunning Jr., *J. Chem. Phys.*, 1989, **90**, 1007; (*c*) A. K. Wilson, D. E. Woon, K. A. Peterson and T. H. Dunning Jr., *J. Chem. Phys.*, 1999, **110**, 7667; (*d*) A. D. Becke, *J. Chem. Phys.*, 1993, **98**, 5648; (*e*) C. Lee, W. Yang and R. G. Parr, *Phys. Rev. B: Condens. Matter Mater. Phys.*, 1988, **37**, 785; (*f*) P. J. Stephens, F. J. Devlin, C. F. Chabalowski and M. J. Frisch, *J. Phys. Chem.*, 1994, **98**, 11623; (*g*) S. H. Vosko, L. Wilk and M. Nusair, *Can. J. Phys.*, 1980, **58**, 1200.

14 (*a*) N. A. Shepelin, Z. P. Tehrani, N. Ohannessian, C. W. Schneider, D. Pergolesi and T. Lippert, *Chem. Soc. Rev.*, 2023, **52**, 2294; (*b*) K. An, H.-N. Lee, K. H. Cho, S.-W. Lee, D. J. Hwang and K.-T. Kang, *Micromachines*, 2020, **11**, 88; (*c*) Z. Zhao, G. Jose, P. Steenson, N. Bamiedakis, R. V. Penty, I. H. White and A. Jha, *J. Phys. D: Appl. Phys.*, 2011, **44**, 095501.